Electronic Supplementary Material (ESI) for Environmental Science: Nano.
This journal is © The Royal Society of Chemistry 2018

Electronic Supplementary Information

Capacitive deionization of saline water using sandwich-like nitrogen-doped graphene composites via a self-assembling strategy

Tingting Yan[a,c], Juan Liu[a], Hong Lei[a], Liyi Shi[a], Zhongxun An[a,b], Ho Seok Park[c] and Dengsong Zhang[a,*]

[a] *Research Center of Nano Science and Technology, Department of Chemistry, College of Sciences, Shanghai University, Shanghai 200444, China*

[b] *National Engineering Research Center of Ultracapacitor System for Vehicles, No. 188 Guo Shou Jing Road, Shanghai 201207, China*

[c] *School of Chemical Engineering, Samsung Advanced Institute for Health Science & Technology (SAIHST), SKKU Advanced Institute of Nano Technology (SAINT), Sungkyunkwan University (SKKU), Suwon 440-746, Republic of Korea*

**Corresponding authors: E-mail: dszhang@shu.edu.cn. Tel: +86-21-66137152*

There are 12 pages including this page, with 4 Tables, and 4 Figures.

Table of Contents

1. Characterization

The morphologies were examined by TEM (JEOL, JEM-200CX) and SEM (JEOL, JEM-700F) .and powdered samples were dispersed in ethanol by ultrasonication for 10 min in an ultrasonic bath. X-Ray diffraction (XRD) measurements were taken on a Rigaku D/MAX-RB X-ray diffractometer using Cu Kα radiation (40kV, 30 20 mA) and a secondary beam graphite monochromator The Raman spectra were recorded on a spectrometer (JY H800UV) equipped with an optical microscope at room temperature. For excitation, the 633 nm line from a HeNe ion laser (Spectra Physics) was focused; with an analyzing spot of about 1 mm, on 35 the sample under the microscope. Nitrogen sorption isotherms were measured with an Autosorb-IQ2, Quantachrome Corporation at 77 K. Before the measurements, all samples were degassed overnight at 593 K in a vacuum line. The Brunauer–Emmett–Teller (BET) method was utilized to calculate the specific surface areas. The X-ray photoelectron spectroscopy (XPS) was recorded on a Perkin-Elmer PHI 5000C ESCA system equipped with a dual X-ray source, using the 45 MgKα (1253.6 eV) anode and a hemispherical energy analyser. The back-ground pressure during data acquisition was kept below 10−6 Pa. All binding energies were calibrated using contaminant carbon (C 1s = 284.6 eV) as a reference.

2. Electrochemical test and batch mode CDI experiments

The cyclic voltammetry (CV) and electrochemical impedance spectroscopy (EIS) were taken on a CHI 660D workstation. CV curves of different nitrogen-doped graphene composite electrodes were measured using a 2-electrode system in a 500 mg/L NaCl aqueous solution. The CV curves of GR/NMC-15 composites at different scan rates and all the EIS measurement were carried out in a 0.5 M NaCl aqueous solution using a three-electrode cell including active materials as working electrode, graphite as the counter electrode, and saturated calomel electrode as the reference electrode, respectively. The specific capacitances were obtained according to the following equation:

$$C = (\int I\, dV)/2vm\Delta V \quad (1)$$

where C is the specific capacitance, I is the response the current, dV is the potential window, v is the sweep rates, and m is the mass of the electrodes.

The CDI electrodes were fabricated by mixing 80 wt.% of the active component, 10 wt.% Super P, 10 wt.% of polytetrafluoroethylene were stirred homogenously, and then the ethanol was added into the mixture. The elastic materials were obtained with the ethanol volatilization and pressed onto graphite sheets by hand pressing and dried at above 110 ^{o}C overnight. To avoid the electrode cracking, electrode materials should be mixed homogeneously and pressed repeatedly. The CDI performance of electrodes was measured in a batch mode experiment, which was conducted in a continuous recycling system as shown in our previous publication [1, 2]. The CDI system herein included

two sided electrodes separated by an insulated spacer. The total active mass of CDI electrode material is 160 mg with a size of 60 mm × 60 mm × 0.1 mm. The NaCl aqueous solution with a total volume of 50 mL was supplied to the cell using a pump with a flow rate of 40 mL min^{-1}. The concentration change of was measured by connecting a conductivity meter (Mettler-Toledo, SevenMulti) at the outlet of the cell, where the solution was released. The beginning concentration of NaCl aqueous solution ranges from 300 to 500 mg L^{-1} with the applied voltage ranging from 1.0 to 1.4 V. The electrosorption capacity of electrodes was calculated according to the following equation:

$$SAC = (C_0 - C)V/m \quad (2)$$

where SAC is salt adsorption capacity, C_0 and C are the initial and final concentrations, and V is the total volume of the NaCl aqueous solution. Meanwhile, m represents the total mass of the electrodes.

$$SAR = SAC/t \quad (3)$$

where SAR represents the salt adsorption rate, t stands for the adsorption time and SAC refers to the salt adsorption capacity.

The charge efficiency (Λ) is described according to the following equation:

$$\Lambda = F \times \Gamma/\sum \quad (4)$$

where F is the Faraday constant (96485 C mol-1), Γ is the salt adsorption capacity (mol g-1) and Σ (charge, C g^{-1}) is obtained by integrating the corresponding current.

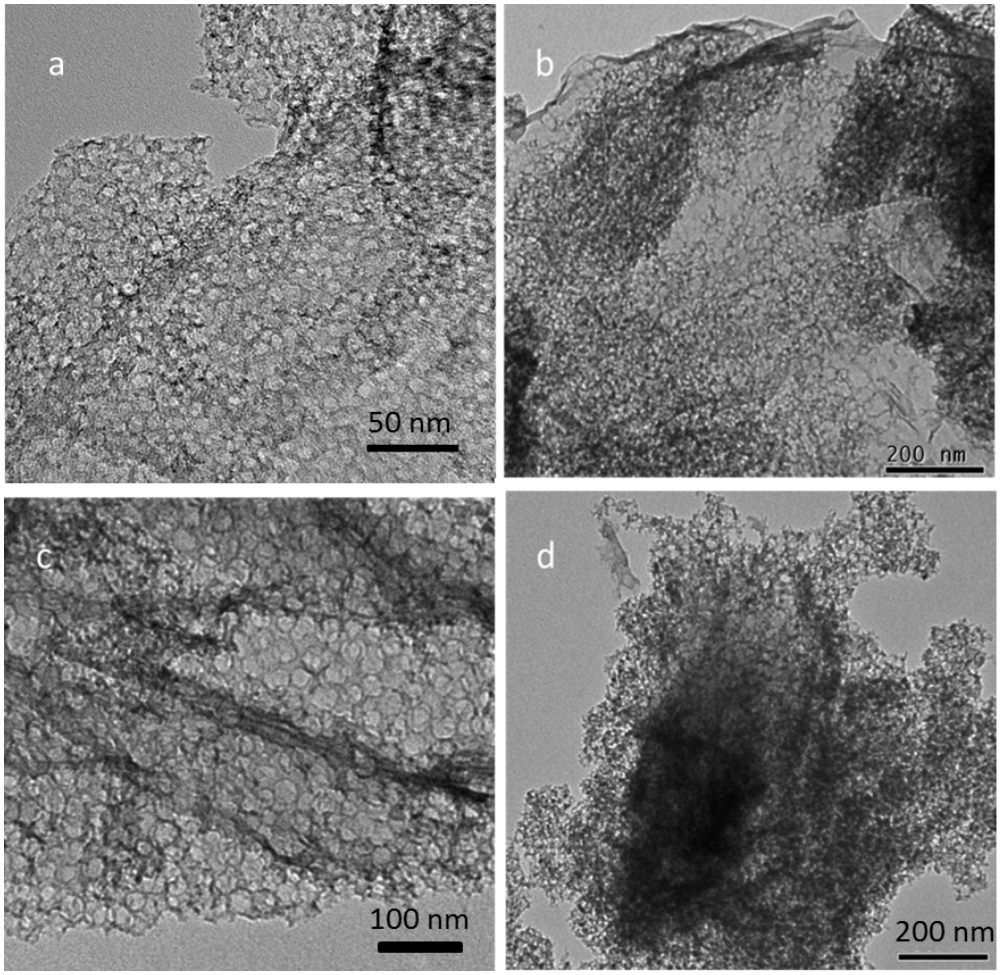

Figure S1. TEM images of (a) GR/NMC, (b) GR/NMC-5, (c) GR/NMC-20, and (d) GR/NMC-30.

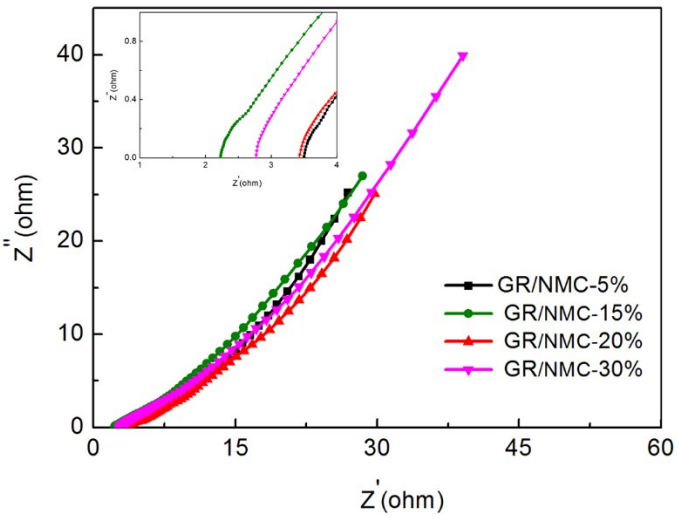

Figure S2 Full EIS spectra of the different samples. The inset is the enlarged view of the high frequency region.

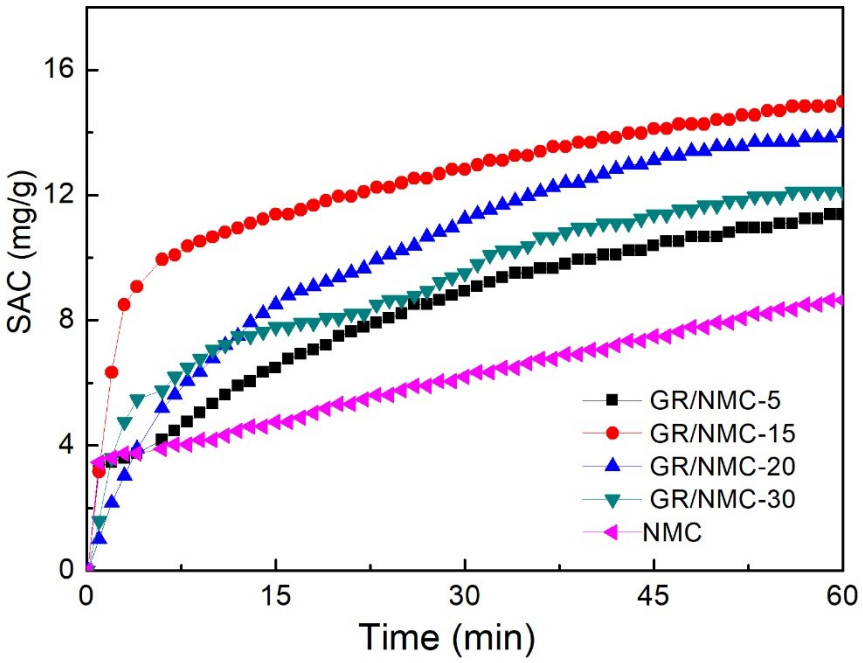

Figure. S3 Plots of SAC vs. time of nitrogen-doped graphene composite and NMC electrodes in a 500 mg/L NaCl aqueous solution at 1.2V.

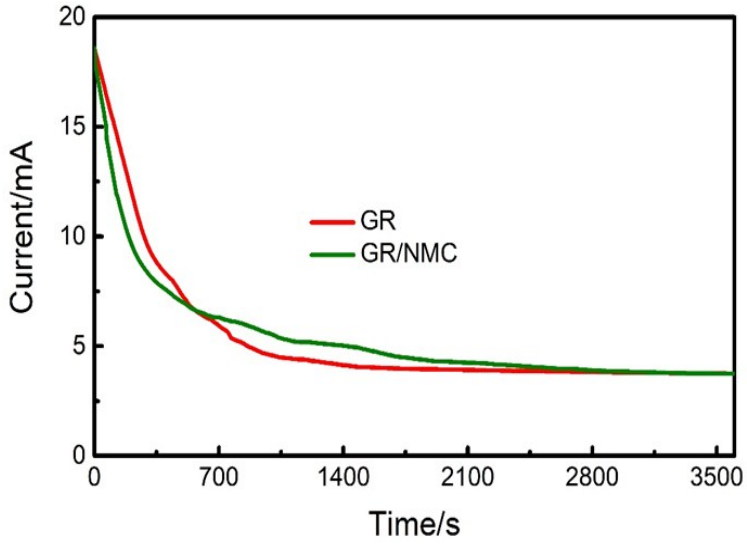

Figure S4. Current transient of GR and GR/NMC electrodes in a 500 mg/L NaCl solution.

Table S1 Chemical compositions of the nitrogen-doped graphene composites from XPS.

Sample	C_{1s} (at%)	N_{1s} (at%)	O_{1s} (at%)
GR/NMC -5	75.75	0.42	24.33
GR/NMC -15	84.07	2.11	13.82
GR/NMC -20	84.20	2.40	13.40
GR/NMC -30	85.37	3.19	11.44

Table S2 The summary of N species for various samples

Samples	Pyridinic N (at%)	Pyrrolic N (at%)	Graphitic N (at%)	Oxidized N (at%)
GR/NMC -5	0.21	0.39	0.22	0.18
GR/NMC -15	0.16	0.39	0.37	0.08
GR/NMC -20	0.22	0.25	0.36	0.17
GR/NMC -30	0.23	0.32	0.21	0.24

Table S3 Specific surface area, pore size and pore volume for the investigated samples.

Sample	Specific surface area ($m^2 g^{-1}$)	Average pore size (nm)	Pore volume ($cm^3 g^{-1}$)
GR	193	5.8	0.60
GR/NMC-5	282	12.4	0.99
GR/NMC-15	918	33.8	2.41
GR/NMC-20	637	48.1	2.59
GR/NMC-30	486	51.4	3.43

Table S4 Comparison of SAC of various carbon electrode materials from the literature.

Electrode materials	Voltage [V]	Initial NaCl concentration [mg L^{-1}]	SAC [mg g^{-1}]	Ref.
3D hierarchical graphene	1.2	500	14.7	3
Mesoporous graphene	1.6	~500	15.2	4
Mesoporous graphene	1.2	500	14.2	5
N-doped carbon aerogel	1.5	~1463	8.2	6
3DNGR–3DSGR	1.4	500	13.72	7
Bi-ZIF-derived Carbon	1.4	500	16.63	8
3D porous graphene	1.4	300	8.97	9
3D graphene	1.4	500	9.48	7
Carbon polyhedron/nanotubes	1.4	500	7.08	10
N-doped carbon/graphene	1.2	589	17.52	11
P-doped carbon aerogels	1.2	500	13.7	12
N-doped multiyolk@shell carbon	1.4	500	16.1	13
Nitrogen-doped porous carbon	1.4	500	16.6	8
N-doped cluster-like porous carbons	1.6	500	17.2	14
N-doped porous carbon spheres	1.2	1000	14.9	15
GR/NMC	1.4	500	18.4	This work
GR/NMC	1.2	500	14.5	This work

References

1. Z. U. Khan, T. Yan, L. Shi and D. Zhang, Improved Capacitive Deionization by Using 3D Intercalated Graphene Sheet-Sphere Nanocomposite Architectures, *Environ. Sci-Nano.*, 2018, **5**, 980-991.
2. H. Y. Duan, T. T. Yan, G. R. Chen, J. P. Zhang, L. Y. Shi and D. S. Zhang, A facile strategy for the fast construction of porous graphene frameworks and their enhanced electrosorption performance, *Chem. Commun.*, 2017, **53**, 7465-7468.
3. H. Wang, T. Yan, P. Liu, G. Chen, L. Shi, J. Zhang, Q. Zhong and D. Zhang, In situ creating interconnected pores across 3D graphene architectures and their application as high performance electrodes for flow-through deionization capacitor, *J. Mater. Chem. A*, 2016, **4**, 4908-4919.
4. X. Gu, M. Hu, Z. Du, J. Huang and C. Wang, Fabrication of mesoporous graphene electrodes with enhanced capacitive deionization, *Electrochim. Acta*, 2015, **182**, 183-191.
5. X. Xu, Y. Liu, M. Wang, X. Yang, C. Zhu, T. Lu, R. Zhao and L. Pan, Design and fabrication of mesoporous graphene via carbothermal reaction for highly efficient capacitive deionization, *Electrochim. Acta*, 2016, **188**, 406-413.
6. G. Rasines, P. Lavela, C. Macías, M. C. Zafra, J. L. Tirado, J. B. Parra and C. O. Ania, N-doped monolithic carbon aerogel electrodes with optimized features for the electrosorption of ions, *Carbon*, 2015, **83**, 262-274.
7. P. Liu, H. Wang, T. Yan, J. Zhang, L. Shi and D. Zhang, Grafting sulfonic and amine functional groups on 3D graphene for improved capacitive deionization, *J. Mater. Chem. A*, 2016, **4**, 5303-5313.
8. Z. Wang, T. T. Yan, J. H. Fang, L. Y. Shi and D. S. Zhang, Nitrogen-doped porous carbon derived from a bimetallic metal-organic framework as highly efficient electrodes for flow-through deionization capacitors, *J. Mater. Chem. A*, 2016, **4**, 10858-10868.
9. A. G. El-Deen, R. M. Boom, H. Y. Kim, H. Duan, M. B. Chan-Park and J. H. Choi, Flexible 3D Nanoporous Graphene for Desalination and Bio-decontamination of Brackish Water via Asymmetric Capacitive Deionization, *ACS Appl Mater Interfaces*, 2016, **8**, 25313-25325.
10. T. Gao, F. Zhou, W. Ma and H. Li, Metal-organic-framework derived carbon polyhedron and carbon nanotube hybrids as electrode for electrochemical supercapacitor and capacitive deionization, *Electrochim. Acta*, 2018, **263**, 85-93.
11. M. Wang, X. T. Xu, J. Tang, S. J. Hou, M. S. A. Hossain, L. K. Pan and Y. Yamauchi, High performance capacitive deionization electrodes based on ultrathin nitrogen-doped carbon/graphene nano-sandwiches, *Chem. Commun.*, 2017, **53**, 10784-10787.
12. Y. Li, Y. Liu, M. Wang, X. Xu, T. Lu, C. Q. Sun and L. Pan, Phosphorus-doped 3D carbon nanofiber aerogels derived from bacterial-cellulose for highly-efficient capacitive deionization, *Carbon*, 2018, **130**, 377-383.
13. H. Wang, T. T. Yan, L. Y. Shi, G. R. Chen, J. P. Zhang and D. S. Zhang, Creating Nitrogen-Doped Hollow Multiyolk@Shell Carbon as High Performance Electrodes for Flow -Through Deionization Capacitors, *ACS Sustain. Chem. Eng.*, 2017, **5**, 3329-3338.
14. Y. Li, Y. Liu, J. Shen, J. Qi, J. Li, X. Sun, J. Shen, W. Han and L. Wang, Design of nitrogen-doped cluster-like porous carbons with hierarchical hollow nanoarchitecture and their enhanced performance in capacitive deionization, *Desalination*, 2018, **430**, 45-55.
15. Y. Liu, T. Q. Chen, T. Lu, Z. Sun, D. H. C. Chua and L. K. Pan, Nitrogen-doped porous carbon spheres for highly efficient capacitive deionization, *Electrochim. Acta*, 2015, **158**, 403-409.